

# Alternating the Crystalline Structural Transition of Coronene Molecular Overlayers on Ag(110) through Temperature Increase

Dongxia Shi,<sup>†</sup> Wei Ji,<sup>†</sup> Bing Yang,<sup>†</sup> Huanyao Cun,<sup>†</sup> Shixuan Du,<sup>†</sup> Lifeng Chi,<sup>‡</sup> Harald Fuchs,<sup>‡</sup> Werner A. Hofer,<sup>§</sup> and Hong-Jun Gao<sup>\*,†</sup>

*Institute of Physics, Chinese Academy of Sciences, P.O. Box 603, Beijing 100190, People's Republic of China; Physics Institute and Center for Nanotechnology (CeNTech), University Muenster, Muenster D-48149, Germany; and Surface Science Research Centre, The University of Liverpool, Liverpool L69 3BX, Britain*

*Received: March 18, 2009; Revised Manuscript Received: July 8, 2009*

By precise control of substrate temperature, two kinds of structures (structure I and structure II) of coronene on Ag(110) are alternately observed by in situ molecular beam epitaxy–low energy electron diffraction. This series of alternating structural transition is confirmed by scanning tunneling microscopy images and density functional theory calculations. As the substrate temperature increases after the molecular monolayer growth at 250 K, the first transition from structure I to structure II occurs around 335 K, which is due to the different vibrational contributions of structures I and II to their free energy. The second transition from structure II to structure I around 367 K is due to the molecule–molecule repulsion, at that temperature the molecular island dissociation and the molecular desorption are dramatically activated and thus the molecule–molecule interaction becomes the dominant effect to the molecular structure. Comprehension of the underlying physics processes behind this alternating structural transition helps establish an understanding of the structural evolution and thermal stability of functional molecular thin films.

## 1. Introduction

The thin films of organic  $\pi$ -conjugated molecules on metal surfaces are excellent prototype systems for investigating controllable fabrications of nanostructures and devices.<sup>1–13</sup> One of the most attractive properties of thin films is based on their controllable and reproducible fabrication of ordered molecular nanostructures, which raises their importance and interest for the control of molecular ordering. In recent studies, the structures of molecular overlayers were successfully tuned by several methods: e.g., the chirality of molecules,<sup>5</sup> the width of substrate facets,<sup>10</sup> lateral nonfunctional alkyl,<sup>11</sup> X-ray irradiation,<sup>12</sup> or specially designed surface templates.<sup>14,15</sup> Most of these methods primarily concentrate on the choice of molecules and substrates. However, the substrate temperature essentially determines the rate of surface diffusion, nucleation, dissociation, desorption, and the speed of the structural relaxation of molecules on surfaces. Therefore, fabricating functional molecular thin films by the precise control of temperature is expected to be an important step toward the rational design of molecular nanostructures.

Moreover, the thermal stability of functional organic molecular thin films in electronic devices would play an essential role in the performance and durability of these devices. It is thus important to gauge the thermal stability of molecular thin films. Because of the high thermal motion speed or rate, e.g., diffusion rate, of molecules on substrates, from the technical point of view, the accompanying structural transition of molecular thin films with increasing substrate temperature is difficult to detect. However, with recent instrumental progress,<sup>16</sup> molecular beam

epitaxy (MBE) combined with low energy electron diffraction (LEED) facility can be adopted, allowing observation of the surface ordering evolution in situ and in real time. A study on the structural evolution of a pentacene overlayer on Ag(110) was recently reported using in situ MBE-LEED which showed that no structural transition occurs during heating, until the thin film changes from a molecular solid into a molecular liquid.<sup>8</sup> In this work, we report an in situ MBE-LEED, scanning tunneling microscopy (STM), and density functional theory (DFT) combined investigation of coronene/Ag(110) overlayer fabrication with the substrate temperature at 250 K and the structural evolution of the heated substrate. Apart from pentacene/Ag(110), a series of alternating structural transitions (like A  $\rightarrow$  B  $\rightarrow$  A) has been found by in situ MBE-LEED as the substrate temperature increased after the growth. The two structures found by the LEED were further confirmed by STM. Furthermore, DFT calculations were employed to understand the underlying physics associated with these transitions. It was found that the growth process at 250 K is primarily dominated by the surface diffusion of coronene molecules, in which two kinds of structures occur successively with increasing coverage. The different vibrational contributions to the free energy correspond to the first transition at the early stage of substrate heating. Increasing the substrate temperature higher, the dissociation of molecular islands and the desorption of molecules were drastically activated, which led to the molecule–molecule interaction (repulsion in the present system) appearing to be the dominant effect and resulted in the second transition.

## 2. Experimental and Theoretical Methods

The experiments were carried out in an ultrahigh-vacuum (UHV) chamber with a base pressure below  $3.0 \times 10^{-10}$  mbar. The chamber was equipped with an in situ MBE-LEED described previously in detail<sup>16</sup> and a variable temperature STM (OMICRON, Germany). Ag(110) crystals were cleaned through

\* To whom correspondence should be addressed. Tel.: +86-10-82648035. Fax: +86-10-62556598. E-mail: hjgao@aphy.iphy.ac.cn.

<sup>†</sup> Institute of Physics, Chinese Academy of Sciences.

<sup>‡</sup> Physics Institute and Center for Nanotechnology (CeNTech), University Muenster.

<sup>§</sup> Surface Science Research Centre, The University of Liverpool.

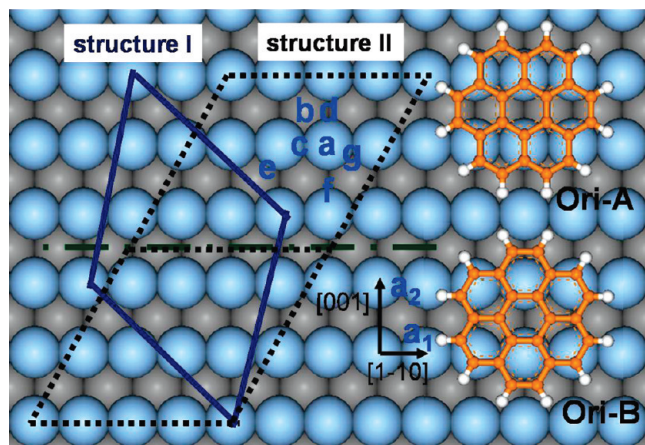


**Figure 1.** Two lattices of structures I (solid line) and II (dotted line), the seven adsorption sites and the two molecular orientations have been considered in DFT calculations.

a standard sputtering with argon ions for 15 min at a pressure of  $5.0 \times 10^{-6}$  mbar and a subsequent annealing procedure at 640 K for 3 min. After that, the Ag(110) surface was checked by LEED. The sublimation temperature of coronene was set at 408 K. The coronene molecules were thoroughly degassed below the sublimation temperature before deposition. Ag(110) crystals were kept at a constant temperature of 250 K during the molecular deposition. The molecular aggregation was monitored in situ by LEED. After deposition, the substrates were heated by an inner filament in the sample holder. The structural changes of the molecular adsorbate during the substrate heating period were monitored in situ by LEED as well. All LEED patterns were taken at an electron beam energy of 13 eV. Subsequently, the surface structures were analyzed by the variable temperature STM. Tungsten tips made by chemically etched tungsten wire with diameter of 0.18 mm were used for STM scanning.

The DFT calculations were carried out using the Perdew–Wang (PW91) generalized gradient approximation (GGA) for the exchange–correlation energy,<sup>17</sup> Projector Augmented Wave (PAW) potentials,<sup>18</sup> and a plane wave basis set as that implemented in the VASP.<sup>19</sup> The Ag(110) surface was modeled using a six-layer slab, separated by a vacuum layer of twelve Ag layers. The calculated equilibrium lattice constant is 4.17 Å. Only the  $\Gamma$  point was used in sampling the surface Brillouin zone. The kinetic energy cutoff for the plane wave basis was up to 400 eV. The coronene molecules were only put on one side (top side) and a dipole correction was applied. According to the LEED data, two lattices have been adopted for structures I and II in Figure 1. The one for structure I contains 11 Ag atoms per supercell, as shown by solid lines, including only one molecule. Since a fractional matrix element exists in the notation matrix of structure II, a supercell containing only one molecule cannot satisfy the periodic boundary condition. Therefore, a supercell including 20 Ag atoms covered by two molecules was adopted to model structure II, as shown by the dotted lines in Figure 1. Seven adsorption sites (a–g) with respect to the center of the molecule were considered, as well as two molecular orientations (Ori-A and Ori-B). In structural relaxations, all atoms except the three bottom Ag layers were fully relaxed until the net force on every atom was less than 0.01 eV/Å.

The Helmholtz free energy was calculated to analyze the evolution of the LEED patterns and the physics of the structural transition under variable temperatures.<sup>20</sup> The Helmholtz free

energy contains, apart from the on-site interaction of single molecules, only two relevant terms: the molecule–molecule interaction, and the entropic contributions due to the excitation of atomic vibrations, since the temperature range is well below 1 eV, or the typical energy scale for excitations is out of the electronic groundstates. Consequently, the Helmholtz free energy ( $F$ ) can be denoted by the following equation, which is a function of independent volume ( $V$ ) and temperature ( $T$ ):<sup>20</sup>

$$F(V, T) = E(V) + F_{\text{vib}} = E(V)_{\text{mol-sub}} + E(V)_{\text{mol-mol}} + \frac{1}{2} \sum_{j,q} \hbar \omega_j(q) + k_B T \sum_{j,q} \ln \left[ 1 - \exp \left[ -\frac{\hbar \omega_j(q)}{k_B T} \right] \right] \quad (1)$$

Here,  $E$  is the static contribution to the internal energy, including two parts  $E_{\text{mol-sub}}$  (molecule–substrate contribution) and  $E_{\text{mol-mol}}$  (molecule–molecule contribution). Both terms were easily accessible by the standard DFT calculation.  $F_{\text{vib}}$  represents the vibrational contribution to the Helmholtz free energy, and  $\omega_j(q)$  is the frequency of  $j_{\text{th}}$  phonon mode at the wave vector  $q$  in the Brillouin Zone (BZ).<sup>20</sup> The vibrational frequencies were calculated by a direct force constant approach implemented in VASP.<sup>21</sup> Systematic independent atomic displacements of 0.02 Å, from the equilibrium in  $x$ ,  $y$ , and  $z$  directions, were applied to obtain the Hellmann–Feynman forces<sup>22,23</sup> of these distorted structures. The dynamical matrix was constructed only for the coronene molecule as an approximation, due to the restricted computer time. Vibrational modes for motion between the molecule atoms and the substrate atoms were not taken into account in view of the relatively weak molecule–substrate interaction and the relatively large mass of the substrate Ag atoms. These modes basically do not significantly influence the energetic contrast between the different structures.

### 3. Results and Discussion

Figure 2a–d shows the LEED pattern evolution of coronene molecules with coverage increase during the deposition. At a low coverage, it presented a halo-like diffuse pattern (Figure 2a) corresponding to a two-dimensional gas state. When the coverage increased, it changed to a ring-like pattern (Figure 2b) corresponding to a two-dimensional liquid state. And when the coverage further increased, 12 sharp spots representing a two-dimensional crystal structure were observable (Figure 2c). Finally, a different pattern (Figure 2d) containing 18 sharp spots was obtained when the coverage reached 1 monolayer (ML). The deposition process was stopped immediately after the pattern in Figure 2d was completed.

By careful analysis of the LEED patterns, it becomes clear that the structure in Figure 2c contains two equivalent domain orientations, symmetric along the [001] axis. This structure, in matrix notation,

$$\begin{pmatrix} 3 & -2 \\ 1 & 3 \end{pmatrix}$$

is a structure, labeled here as structure I. Similarly, the pattern in Figure 2d is a mixture of structure I and another structure, namely,

$$\begin{pmatrix} 4 & 0 \\ 2 & 2.5 \end{pmatrix}$$

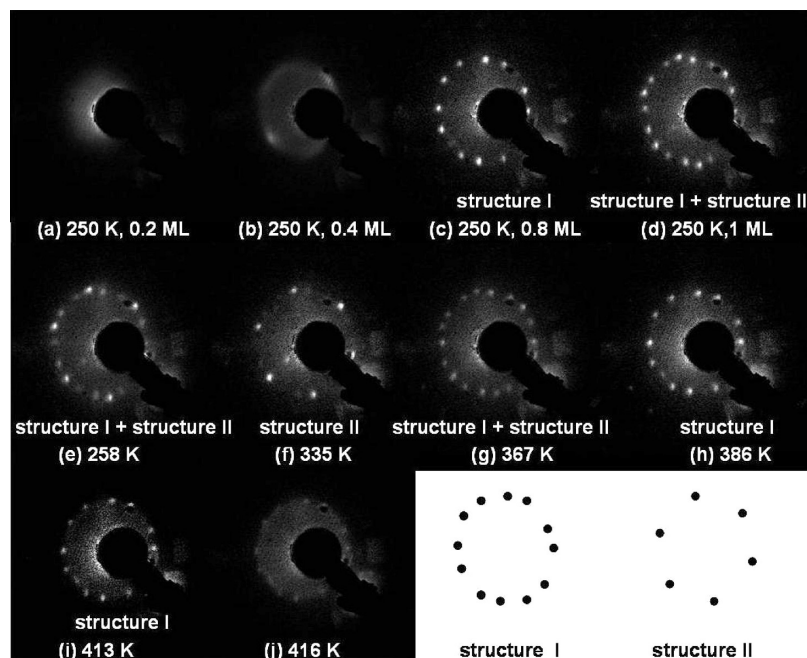


**Figure 2.** LEED images of coronene adsorbed on Ag(110) with the increase of coverage parts a–d and with a further increase of the substrate temperature e–j. Insets are sketches of the LEED patterns of structures I and II.

labeled as structure II. It is clear that the structural evolution from Figure 2c (structure I) to Figure 2d (structure I + structure II) is coverage dependent. In the early stage of the evaporation process, the low-coverage favored structure I is dominant (Figure 2c). As the coverage increases, the density of the molecules on the substrate increases, imposing constraints on the molecular diffusion. Newly adsorbed molecules at this point do not have sufficient time to relax their relatively high kinetic energy (energy introduced by evaporation) reaching their equilibrium structure at that temperature. The lack of diffusion thus leads to the appearance of a more compact structure II, which agrees with the found coexistence of structures I and II at 1 ML coverage (Figure 2d).

These two structures derived from the LEED were confirmed by STM and DFT. In the STM experiment, two mirror domain orientations of structure I were observed (Figure 3a), but only one domain orientation of structure II (Figure 3b) was observed, which is consistent with the surface symmetry of the two supercells (Figure 1). The STM images shown here are scanned at room temperature. In terms of the DFT calculation, 20 individual configurations have been considered, searching for the most likely groundstate adsorption configuration. For structure I, the calculation indicates that both sites **c** and **g** are energetically favored, within an energy difference of less than 5 meV, close to the limit of accuracy in DFT. Similar results were obtained for structure II where the most likely configuration is the molecule adsorbed at site **g**, according to the noninteger element in the lattice matrix of structure II. The fully relaxed geometries of structures I and II are shown in Figure 3, parts c and d, in which the molecules have a small rotation of  $\sim 6^\circ$  with respect to the two unit cell vectors of the substrate lattice, and the averaged molecule–molecule distances are 12.5 and 11.8 Å for structures I and II, respectively. According to the experimental measurement, the average intermolecular distances are 12.25 and 11.65 Å for structures I and II, respectively, which are consistent with the DFT calculation.

During the deposition, the substrate temperature was kept constant at 250 K. Structures I and II occurred successively with coverage increase. However, they showed up simultaneously

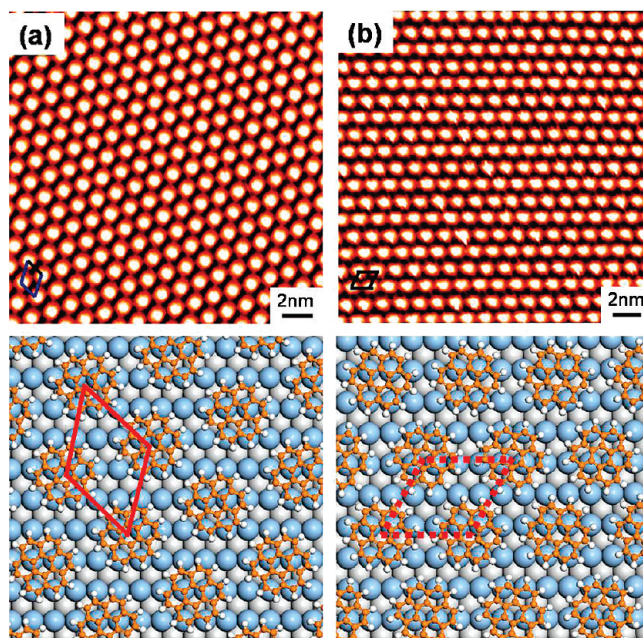


**Figure 3.** Parts a and b, STM images of structures I and II, respectively (Scanning parameters: area = 22 nm × 22 nm,  $V = -1.12$  V,  $I = 0.08$  nA), the unit cells of structures I and II are marked separately in the bottom-left of the images. Parts c and d, the calculated fully relaxed configurations of structures I and II, respectively, the unit cells are marked.

with the coverage increase during deposition if the substrate temperature was kept at room temperature.<sup>16</sup> It strongly suggests that structure I is a surface-diffusion and low-temperature favored structure. This also begs the question of whether the structure in Figure 2d (structure I + structure II) is the final stable structure. Therefore, we heated the substrate after the complete deposition to determine the influence of temperature on the molecular overlayer structures. Interestingly, coronene molecules adsorbed on Ag(110) displayed an alternating structural transition in the period of substrate heated, discussed as follows.

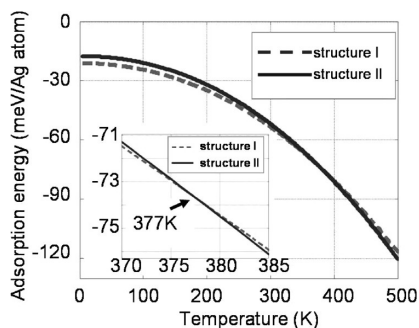


**Figure 4.** Calculated free energies of structures I and II versus temperature. For a dense molecular overlayer, structure I is favored from 0 to 377 K, structure II is favored above 377 K. The inset shows the zoomed-in curves between 370 and 385 K.

The evolution of LEED patterns with the heated substrate is shown in Figure 2e–j. As the substrate temperature increased, the spots corresponding to structure I gradually faded away (Figure 2e). Only the diffraction pattern of structure II was observable when the substrate was heated to 335 K (Figure 2f). However, structure I reappeared when the substrate temperature was raised to 367 K, where the two structures coexisted as shown in Figure 2g. After that, structure II disappeared and only structure I existed when the temperature increased to 386 K (Figure 2h). There was no further structural transition at higher temperatures, but the LEED spots of structure I diffused gradually as the temperature was raised to 413 K (Figure 2i) and finally disappeared at 416 K (Figure 2j).

The decisive variable for a thermodynamic description of the system is the Helmholtz free energy  $F$  described previously, which provides a quantitative understanding of structural transition at a finite temperature.<sup>20</sup> According to eq 1, the calculated free energies of structures I and II as functions of temperature for a dense molecular overlayer are displayed in Figure 4, which illustrates the different free energies per substrate atom between the two structures with the change of temperatures. It was found that at a temperature below 377 K, structure I is energetically favored. However, at a temperature higher than 377 K, the effect of vibrational contributions stands out and structure II is energetically favored due to the different vibrational contributions of structures I and II to their free energies.

The finding of the Helmholtz free energy calculation is actually shared by the LEED experiment. As the substrate temperature increased from 250 to 335 K (Figure 2d–f), structure I changed into structure II, implying a structural transition around 335 K. Considering that the low dimension and the defects can usually lower the critical temperature of a structural transition, it is thus very reasonable that the observed transition happens at a temperature tens of Kelvin lower than the predicated critical temperature (377 K) based on an ideal crystal. Actually, the molecular adsorbates are basically all in solid–liquid (gas) phase equilibria in UHV chambers. At a relatively low temperature, almost all coronene molecules are in a solid phase. In this case, the transition from structure I to structure II (Figure 2d–f) can be well explained by the calculated free energies shown in Figure 4. However, as the substrate temperature increases beyond 367 K (Figure 2g), the relatively low adsorption energy of coronene in a 2D crystal ( $\sim -0.25$  eV) leads to the dissociation of molecular islands and the desorption of a small amount of molecules. In this way, the term  $E_{\text{mol-mol}}$  contributing to the total free energy,  $F$ , stands out and becomes the dominant effect, which can hardly be

reflected in Figure 4, since the volume and/or area of the adsorbed molecules varies.

At high temperature, the molecule–molecule interaction is much more important than the molecule–substrate interaction. So we only consider the molecule–molecule interaction without the substrate. The calculated molecular interaction energies are 0.10 eV for structure I and 0.13 eV for structure II, respectively, which means the interactions between molecules in these lattices are repulsive if the substrate is not considered. The energy difference between these two structures is 0.03 eV. It indicates that the looser structure I is more favorable than structure II without substrate. This is in agreement with the experiment that only structure I is observed at high temperatures. The repulsive molecule–molecule interaction offers a reasonable explanation to the structural transition from structure II to structure I at the higher temperatures (Figure 2g–h).

#### 4. Conclusions

The structure of coronene molecules adsorbed on Ag(110) has been investigated. Two structures, say I and II, occurred successively with the increase in coverage. A series of alternating structural transitions between these two structures has been found as the substrate temperature increased after growth. In particular, a transition from structure I to structure II was found at around 335 K, and another transition from structure II to structure I was found at around 367 K. It turns out that the first transition is due to the fact that the vibrational term of structures I and II contribute differently to their free energies. Structure I is energetically favored below 335 K and structure II is favored above 335 K, based on the LEED observation (377 K based on the DFT prediction using an ideal crystal). Increasing the substrate temperature over 367 K (according to the LEED data), the process of the molecular island dissociation and the molecule desorption are drastically activated. The molecule–molecule interaction (repulsion in present system) thus stands out and dominates the molecular structure at that temperature, leading to the second transition from structure II to structure I. An understanding of temperature-induced structural transitions provides us a reference point to avoid malfunction of molecular devices working at high temperatures. The subtle interplay found to exist among these factors, e.g., diffusion, free energy, dissociation, and desorption, reminds us that it is possible to fabricate desired molecular structures by changing the sample temperature before, during, or after the molecular deposition.

**Acknowledgment.** This work was partially supported by the Natural Science Foundation of China (NSFC), the MOST 973 and 863 projects of China, the Chinese Academy of Sciences (CAS), Supercomputing Center, CNIC, CAS, Shanghai Supercomputer Center, and the Collaborative Research Centre TRR 61.

#### References and Notes

- (1) Yokoyama, T.; Yokoyama, S.; Kamikado, T.; Okum, Y.; Mashiko, S. *Nature (London)* **2001**, *413*, 619.
- (2) Rosei, F.; Schunack, M.; Jiang, P.; Gourdon, A.; Lagsgaard, E.; Stensgaard, I.; Joachim, C.; Besenbacher, F. *Science* **2002**, *296*, 328.
- (3) Theobald, J. A.; Oxtoby, N. S.; Philipps, N. A.; Champness, N. R.; Beton, P. H. *Nature (London)* **2003**, *424*, 1029.
- (4) Gao, H.-J.; Sohlberg, K.; Xue, Z. Q.; Chen, H. Y.; Hou, S. M.; Ma, L. P.; Fang, X. W.; Pang, S. J.; Pennycook, S. J. *Phys. Rev. Lett.* **2000**, *84*, 1780. Shi, D. X.; Song, Y. L.; Zhu, D. B.; Zhang, H. X.; Jiang, P.; Xie, S. S.; Pang, S. J.; Gao, H.-J. *Adv. Mater.* **2001**, *13*, 1103.
- (5) Stepanow, S.; Lin, N.; Vidal, F.; Landa, A.; Ruben, M.; Barth, J. V.; Kern, K. *Nano Lett.* **2005**, *5*, 901.

- (6) Reuter, K.; Stampfl, C.; Scheffler, M. In *Handbook of Materials Modeling*; Yip, S., Ed.; Springer: Berlin, 2005.
- (7) Zhang, Y.; Blum, V.; Reuter, K. *Phys. Rev. B* **2007**, *75*, 235406.
- (8) Wang, Y. L.; Ji, W.; Shi, D. X.; Du, S. X.; Seidel, C.; Ma, Y. G.; Gao, H.-J.; Chi, L. F.; Fuchs, H. *Phys. Rev. B* **2004**, *69*, 075408.
- (9) Gao, L.; Deng, Z. T.; Ji, W.; Lin, X.; Cheng, Z. H.; He, X. B.; Shi, D. X.; Gao, H.-J. *Phys. Rev. B* **2006**, *73*, 075424. Gao, L.; Liu, Q.; Zhang, Y. Y.; Jiang, N.; Zhang, H. G.; Cheng, Z. H.; Qiu, W. F.; Du, S. X.; Liu, Y. Q.; Hofer, W. A.; Gao, H.-J. *Phys. Rev. Lett.* **2008**, *101*, 197209.
- (10) Du, S. X.; Gao, H. J.; Seidel, C.; Tsetseris, L.; Ji, W.; Kopf, H.; Chi, L. F.; Fuchs, H.; Pennycook, S. J.; Pantelides, S. T. *Phys. Rev. Lett.* **2006**, *97*, 156105.
- (11) Shi, D. X.; Ji, W.; Lin, X.; He, X. B.; Lian, J. C.; Gao, L.; Cai, J. M.; Lin, H.; Du, S. X.; Lin, F.; Seidel, C.; Chi, L. F.; Hofer, W. A.; Fuchs, H.; Gao, H.-J. *Phys. Rev. Lett.* **2006**, *96*, 226101.
- (12) Ji, W.; Lu, Z.-Y.; Gao, H. *Phys. Rev. Lett.* **2006**, *97*, 246101.
- (13) Ji, W.; Lu, Z.-Y.; Gao, H. -J. *Phys. Rev. B* **2008**, *77*, 113406.
- (14) Fasel, R.; Parschau, M.; Ernst, K.-H. *Angew. Chem., Int. Ed.* **2003**, *42*, 5178.
- (15) Ruffeux, P.; Palotás, K.; Gröning, O.; Wasserfallen, D.; Müllen, K.; Hofer, W. A.; Gröning, P.; Fasel, R. *J. Am. Chem. Soc.* **2007**, *129*, 5007.
- (16) Seidel, C.; Ellerbrake, R.; Gross, L.; Fuchs, H. *Phys. Rev. B* **2001**, *64*, 195418.
- (17) Perdew, J. P. In *Electronic Structure of Solids '91*; Ziesche, P., Eschrig H., Eds.; Akademie Verlag: Berlin, 1992.
- (18) Bläochl, P. E. *Phys. Rev. B* **1994**, *50*, 17953. Kresse, G.; Joubert, D. *Phys. Rev. B* **1999**, *59*, 1758.
- (19) Kresse, G.; Furthmüller, J. *Phys. Rev. B* **1996**, *54*, 11169. Kresse, G.; Hafner, J. *Phys. Rev. B* **1993**, *47*, R558.
- (20) Wallace, D. C. *Thermodynamics of Crystals*; Wiley: New York, 1972.
- (21) Kresse, G.; Furthmüller, J.; Hafner, J. *Europhys. Lett.* **1995**, *32*, 729.
- (22) Hellmann, H. *Einführung in die Quantenchemie*; Franz Deuticke: Leipzig, 1937; p 285.
- (23) Feynman, R. P. *Phys. Rev.* **1939**, *56*, 340.

JP902416R